

Original Article



Trans-chalcone induces death by autophagy mediated by p53 up-regulation and β -catenin down-regulation on human hepatocellular carcinoma HuH7.5 cell line

Elaine da Silva Siqueira^{a,*}, Vrgnia Mrcia Concato^a, Fernanda Tomiotto-Pellissier^{a,b}, Taylon Felipe Silva^a, Bruna Taciane da Silva Bortoleti^{a,b}, Manoela Daiele Gonalves^c, Idessania Nazareth Costa^a, Waldiceu Aparecido Verri Junior^d, Wander Rogrio Pavanelli^a, Carolina Panis^e, Mrio Srgio Mantovani^f, Milena Menegazzo Miranda-Sapla^a, Ivete Conchon-Costa^a

^a Laboratory of Immunopathology of Neglected Diseases and Cancer, State University of Londrina – UEL. Rodovia Celso Garcia Cid Campus Zip Code 86057-970, Post Box 10.011. Londrina, PR, Brazil

^b Graduate Program in Biosciences and Biotechnology, Carlos Chagas Institute (ICC), Focruz, Curitiba, Paran, Brazil

^c Laboratory of Biotransformation and Phytochemistry, State University of Londrina, Paran, Brazil

^d Laboratory of Research for Pain, Neuropathy and Inflammation, State University of Londrina, Paran, Brazil

^e Laboratory of Tumor of Biology, State University of West Paran, Francisco Beltro, Paran, Brazil

^f Laboratory of Toxicological Genetics, State University of Londrina, PR, Brazil

ARTICLE INFO

Keywords:

Hepatocellular carcinoma
Trans-chalcone
Autophagy
p53
 β -catenin

ABSTRACT

Background: Hepatocellular Carcinoma (HCC) is extremely aggressive and presents low rates of response to the available chemotherapeutic agents. Many studies have focused on the search for alternative low-cost natural compounds with antiproliferative potential that selectively respond to liver cancer cells.

Purpose: This study assessed the *in vitro* direct action of *trans*-chalcone (TC) on cells of the human HCC HuH7.5 cell line.

Methods: We subjected the HuH7.5 tumor cells to TC treatment at increasing concentrations (12.5–100 μ M) for 24 and 48 h. Cell viability was verified through MTT and 50% inhibitory concentration of cells (IC₅₀ 23.66 μ M) was determined within 48 h. We quantified trypan blue proliferation and light microscopy, ROS production, mitochondrial depolarization and autophagy, cell cycle analysis, and apoptosis using Muse® cell analyzer and immunocytochemical markings of p53 and β -catenin.

Results: Data showed an effective dose- and time-dependent TC-cytotoxic action at low micromolar concentrations without causing toxicity to non-cancerous cells, such as erythrocytes. TC-treatment caused mitochondrial membrane damage and cell cycle G0/G1 phase arrest, increasing the presence of the p53 protein and decreasing β -catenin, in addition, to inducing cell death by autophagy. Additionally, TC decreased the metastatic capacity of HuH7.5, which affected the migration/invasion of this type of cell.

Conclusion: *In vitro* TC activity in the human HCC HuH7.5 tumor cell line is shown to be a potential molecule to develop new therapies to repair the p53 pathway and prevent the overexpression of Wnt/ β -catenin tumor development inducing autophagy cell death and decreasing metastatic capacity of HuH7.5 cell line.

Abbreviations: BSA, bovine serum albumin; CCCP, Carbonyl cyanide *m*-chloro-phenylhydrazone; DAB, 3,3'-diaminobenzidine; DMEM, Dulbecco's modified Eagle's medium; DMSO, dimethylsulfoxide; Doxo, Doxorubicin; FBS, fetal bovine serum; HCC, Hepatocellular Carcinoma; HRP, horseradish peroxidase; IC₅₀, 50% inhibitory concentration; MTT, 3-(4,5-dimethylthiazol-2-yl)-2,5-diphenyltetrazolium bromide; MDC, monodanzylcadaverine; ROS, reactive oxygen species; OD, optical density; PBS, Phosphate-buffered saline; PI, propidium iodide; PS, phosphatidylserine; ROS, reactive oxygen species; TC, *trans*-chalcone; TMRE, tetramethylrhodamine ethyl ester probe.

* Corresponding author.

E-mail address: elaine.siqueira15@hotmail.com (E.S. Siqueira).

<https://doi.org/10.1016/j.phymed.2020.153373>

Received 30 June 2020; Received in revised form 20 August 2020; Accepted 8 October 2020

Available online 9 October 2020

0944-7113/© 2020 Elsevier GmbH. All rights reserved.

Introduction

Hepatocellular carcinoma (HCC) constitutes 75–85% of primary liver tumors, according to the International Agency for Research on Cancer, corresponding to the sixth most prevalent cancer worldwide and the fourth cancer-related cause of death, thus representing a major global public health problem. According to the literature, in 2008 > 694 thousand HCC-related deaths were registered worldwide and in 2018 the mortality rate reached 781 thousand cases (New Global Cancer Data: GLOBOCAN 2018).

Liver transplant is among the most efficient therapies available, and is indicated at the early stage of the disease, followed by surgical resection, ablation, or trans-arterial therapies (Sim and Knox, 2018), in addition to a wide range of anti-tumor drugs. However, as HCC is usually diagnosed at its late phase, systemic chemotherapy treatment is challenging because of its very aggressive nature, which involves low response rates, resistance to multiple drugs, several side effects, and low recovery rate (Zhang et al., 2019). In this context, research has focused on finding improved therapeutic strategies for HCC-related signaling pathways involved in the tumorigenic process.

Although cancer originates from a combination of mutations in oncogenes, developmental pathways, and tumor suppressor genes, it is common to occur p53 mutations in human liver cancer, characterized as typically highly aggressive and resistant to non-surgical therapies (Xue et al., 2007). HCC also displays altered Wnt/ β -catenin signaling in which more than one-third of HCC cases exhibit cytoplasmic and/or nuclear accumulation of β -catenin, which correlates to poor differentiation and prognosis (Wands and Kim, 2014). p53 is an important gene that presents a complex role on tumorigenic suppression by repairing the tumor that restricts proliferation in response to DNA damage or deregulation of mitogenic oncogenes leading to the induction of various cell cycle checkpoints, apoptosis, autophagy, or cellular senescence (Blandino et al., 2020). Aberrant activation of this pathway generates the accumulation of β -catenin in the nucleus and promotes the transcription of many oncogenes, such as c-Myc and CyclinD-1 (Cagatay and Ozturk, 2002).

Therefore, developing gene therapies aimed at repairing the p53 pathway and inducing cell death is extremely promising. In this context, chalcones (1,3-diphenyl-2-propene-1-ones) have been described as a class of substances with antitumor potential for being open-chain precursors for flavonoid biosynthesis and biologically classified as secondary metabolites of low molecular weight (Bonakdar et al., 2017). In most cases, the most stable nature of the isomer is *trans*-chalcone (TC) (1,3-diphenyl-2-propene-1-one) (Aksöz and Ertan, 2011), which has antioxidant, anti-inflammatory properties and inhibits proliferation in different human cancer cell lines by upregulating the tumor suppressor p53 gene (Silva et al., 2018, 2016).

However, considering that the literature is yet to include studies investigating the TC in human HCC HuH7.5 line, this study aimed at investigating the *in vitro* antiproliferative action of this compound as well as elucidating the possible death mechanisms through which TC acts on this tumor cell line.

Materials and methods

Trans-chalcone

Commercial TC, $\geq 97\%$ purity (Fig. 1), was obtained from Santa Cruz Biotechnology, Inc. (Santa Cruz, CA- Catalog Number sc-204,681 - Dallas, USA). Stock solution of TC was dissolved in 1% dimethylsulfoxide (DMSO) (Sigma, St. Louis, MO, USA). DMSO concentration up to 0.02% in all experiments.

Cell culture

HuH7.5 tumor cells grown in DMEM medium (Dulbecco's modified

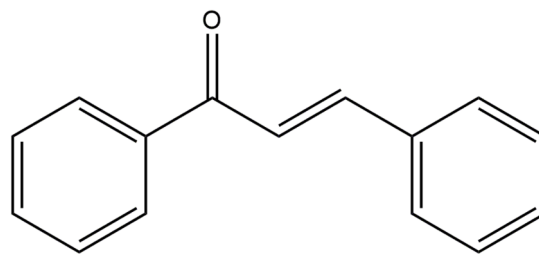


Fig. 1. Chemical structure of *trans*-chalcone (1,3-diphenyl-2-propene-1-one).

Eagle's medium, Lifetechnologies, Carlsbad, CA, USA) supplemented with 10% fetal bovine serum (FBS, Lifetechnologies), 100 U/ml penicillin, and 100 μ g/ml streptomycin (Santa Cruz Biotechnologies, Dallas, TX, USA) and incubated at 37 °C in 5% CO₂.

Cell viability assay

The MTT assay was performed as previously described (Gonçalves et al., 2018). HuH7.5 cells (10⁴ cell/well) were incubated with TC in 96-well plates (12.5, 25, 50, and 100 μ M) or 25 μ M- Doxorubicin (Doxo) (Actavis Italy S.p.A., Pfizer) for 24, 48 and 72 h (37 °C, 5% CO₂). Cells were washed and MTT was added (0.05 mg/ml) with incubation for 3 h. MTT product (formazan crystals) was diluted with 100 μ l of DMSO and read in a spectrophotometer (Thermo Scientific, Multiskan GO) at 540 nm. Cells with DMEM was used as a control, DMSO as vehicle and Doxo (25 μ M/ml) as a positive control. Results were expressed as the percentage of viability in relation to the control group calculated according to the following formula: % (viable cells) = (OD of TC- treated samples / OD control-sample) \times 100. From the data obtained through the MTT assay, the 50% inhibitory concentration of (IC₅₀) curve was calculated using a logarithmic regression.

Trypan blue exclusion cytotoxicity assessment

HuH7.5 cells (3 \times 10⁴ cell/well) were treated with TC-IC₅₀ (23.66 μ M \pm 0.02), as well as after 24 and 48 h incubations (37 °C, 5% CO₂). To assess cell viability, the suspension was diluted in 0.4% trypan blue solution at a 1:1 ratio. We counted the total number of viable and dead cells through light microscopy (Olympus BX41, Olympus Optical Co., Ltd., Tokyo, Japan) fusing a neubauer camera. This assay was performed in triplicate with three independent experiments.

Quantification of HuH7.5 cell number through image microscopy

HuH7.5 cells (10⁶ cell/well) were treated with TC-IC₅₀ (23.66 μ M \pm 0.02) or Doxo (25 μ M) and incubated for 48 h. Photomicrographs (20 \times objective lens) were then performed using an inverted imaging system EVOS™ (Thermo Fisher Scientific®) to analyze cell count after the treatments.

Scratch assay

HuH7.5 cells (10⁶ cell/well) were seeded into 6-well plates and incubated (37 °C, 5% CO₂) until reaching confluence. Subsequently, we generated a scratch in the monolayer by gently passing 200 μ l tip on the bottom of each well, and treated the cells with TC-IC₅₀ (23.66 μ M \pm 0.02) and control (cells supplemented with medium). Photomicrographs (20 \times objective lens) were performed using an EVOS microscope (Life Technologies) at different times (0, 12, 24, and 48 h). We assessed cell migration as a free area (region without cells) measured on the Image-Pro-Plus Program software, while the percentage decrease in the area characterized the cell migration index. Assays were obtained in triplicates from each group tested.

Production of reactive oxygen species (ROS)

To assess the ROS generation, HuH7.5 cells (10^4 cells/well) were treated with TC-IC₅₀ per 4 and 48 h, and the assay was performed as previously described (Concato et al., 2020).

Mitochondrial membrane potential determination ($\Delta\Psi_m$)

$\Delta\Psi_m$ analysis was performed using tetramethylrhodamine-ethyl ester (TMRE) labeling (Sigma, St. Louis, MO, USA). HuH7.5 cells (10^4 cell/well) were treated with TC-IC₅₀ ($23.66 \mu\text{M} \pm 0.02$) for 48 h. The assay was performed as previously described (Concato et al., 2020).

Determination of autophagic vacuoles

For the quantification of autophagic vacuoles, cells (10^4 cell/well) were treated with TC-IC₅₀ ($23.66 \mu\text{M} \pm 0.02$) for 48 h and, the cells were subsequently washed with PBS and incubated with monodansylcadaverine (MDC) ($50 \mu\text{M}$) (Sigma - Aldrich, St. Louis, MO, USA). Data were obtained using a microplate fluorescence reader (Victor X3, PerkinElmer, Finland), with excitation wavelength (380 nm) and emission (525 nm). Experimental groups were defined as described in the cell viability assay.

Analysis of the cell cycle

HuH7.5 cells (2×10^6 cell/well) were seeded in a 6-well plate for 24 h and subsequently treated with TC-IC₅₀ ($23.66 \mu\text{M} \pm 0.02$) and incubated for the same period. Thereafter, the cell suspension was subjected to centrifugation (1500 rpm/5 min) and the cell pellet was resuspended in 300 μl of PBS. Afterward, a solution containing 0.05% ribonuclease A (RNase A) (Sigma, St. Louis, MO, USA) was added and incubated (30 min/37 °C). In the final step, a solution of 0.1% sodium citrate and 1% Triton-X100 was added to 50 $\mu\text{g}/\text{ml}$ propidium iodide (PI) (Sigma, St. Louis, MO, USA) for 30 min. Fluorescence was estimated using a Muse Cell Analyzer (Merck Millipore), with 5000 events. DNA content was analyzed and the percentage values of cells at different phases of the cycle (G0/G1, S, and G2/M) were estimated according to their fluorescence intensity.

Immunocytochemical detection of p-p53 and β -catenin

Slides labeled with streptavidin-biotin using LSAB KIT (DAKO Japan, Kyoto, Japan) were incubated with 10% Triton X-100 solution for 1 h, washed three times in PBS and treated for 40 min at room temperature with bovine serum albumin (BSA) 10% and incubated overnight at 4 °C with primary antibodies β -catenin (1: 500) and p53 (1: 300) (Santa Cruz Biotechnology). After treatment with secondary antibody (2 h, room temperature), we visualized the activity of horseradish peroxidase (HRP) by applying the treatment with H₂O₂ and 3,3'-diaminobenzidine (DAB) for 5 min. Finally, the sections were slightly contrasted with Harry's hematoxylin (Merck). For each case, negative controls were performed omitting the primary antibody. We examined the intensity and location of immunoreactivities against the primary antibody used on all slides through a photomicroscope (Olympus BX41, Olympus Optical Co., Ltd., Tokyo, Japan) (40 \times objective lens). To determine a semi-quantitative score, we evaluated the images using the color deconvolution tool on the Image J software (NIH, USA). The categorization of pixels was performed as previously described Chatterjee et al. (2013) as high positive (3+), positive (2+), low positive (1+), and negative (0).

Cell apoptosis assay

HuH7.5 cells (10^6 cells/well) were treated with TC-IC₅₀ ($23.66 \mu\text{M} \pm 0.02$) for 48 h. After this treatment period, the cell suspension was washed with PBS and 50 μl of Annexin V, and a dead cell kit (Millipore,

Billerica, MA, USA) was added for 20 min at room temperature to determine apoptosis. Samples were analyzed using a flow cytometer Muse Cell Analyzer (Muse® Cell Analyzer, Merck Millipore) and the results were analyzed using the Muse Cell Analyzer™ software.

Statistical analysis

Statistical differences were obtained after analysis of variance (ANOVA), followed by the Tukey test for multiple comparisons using GraphPad Prism 6.01 for Windows (GraphPad Software, San Diego California, USA). Data were expressed as mean \pm standard error of the mean (SEM) and were considered significant differences upon p -value ≤ 0.05 . Values were also categorized as: * ($p \leq 0.05$); ** ($p \leq 0.01$); *** ($p \leq 0.001$); **** ($p \leq 0.0001$).

Results

Antiproliferative effect on cell HuH7.5 and lower metastatic capacity with TC

In order to investigate the cytotoxic effect of TC against HCC HuH7.5 cells, we performed an MTT assay and found that cell viability of the HuH7.5 line treated with TC (12.5; 25; 50 and 100 μM) decreased significantly ($p \leq 0.0001$) at all times tested regarding the control (Fig. 2A, B). At 24 h, higher doses of TC (25; 50 and 100 μM) were more effective as an antiproliferative agent on tumor cells than the positive control (Doxo 25 μM) ($p \leq 0.0001$). In addition, the concentration of 100 μM reduced cell viability in 65.2% in relation to the control, proving the most effective of the tested concentrations (Fig. 2A). TC concentrations (25 and 50 μM) did not differ from each other, reducing cell proliferation in 39.8 and 45.6%, respectively (Fig. 2A). When assessing the effect of TC at 48 h of treatment, we verified a dose- and time-dependent effect at about 24 h, significantly reducing cell viability in 22.6, 64.4, 77.7, 88.6% when treated with TC-concentrations of 12.5, 25, 50 and 100 μM , respectively (Fig. 2B) (Table 1).

At 48 h, there was no significant difference between TC treatment at concentrations 50 and 100 μM and positive control, Doxo 25 μM (Fig. 2B). Subsequently, we determined the IC₅₀ of TC on HuH7.5 cells and, the results showed the IC₅₀ were 53 μM (± 0.04) and 23.66 μM (± 0.02) for 24 h and 48 h, respectively. Thus, as the results were time-dependent, we proceeded with the remaining experiments by applying the concentration of 23.66 μM at the time of 48 h (Table 1), and also because the replicative period of liver tumor cells is 14 to 48 h and mitotic peak at 48 h (Bonakdar et al., 2017). In addition, even regarding the cytotoxicity properties, it is worth mentioning that the TC-concentrations tested had no hemolytic effect on erythrocytes (data not shown).

In order to confirm the results from the MTT assay, we counted the number of viable cells by applying the trypan blue exclusion method. After 48 h of the HuH7.5 cell TC-IC₅₀ treatment, we found that the TC treatment showed a cytotoxic effect that reduced 51.3% of the number of viable cells comparing with the control ($p \leq 0.0001$) – as illustrated in the representative image (Fig. 2D).

Understanding that the ability of tissue migration and invasion is a hallmark of malignant tumor cells, we also analyzed whether the metastatic capacity of the HuH7.5 cell was altered by the TC treatment or by the cell migration assay. The results showed that the control group cells presented a wound closure capacity after 12 - 48 h of culture (Fig 3A, B). TC-IC₅₀ significantly inhibited this metastatic capacity of HuH7.5. After 12 h, only 1% of wound closure occurs, and at 24 h and 48 h, the distance reduction was significantly lower than in the control, reaching only 39.5% and 26.6% of wound closure, respectively (Fig 3A, B).

According to these findings, the *in vitro* TC treatment showed a direct cytotoxic effect on HCC HuH7.5 reducing the main characteristics of cancer cells, cell proliferation, as well as the ability of migration and invasion of this cell line.

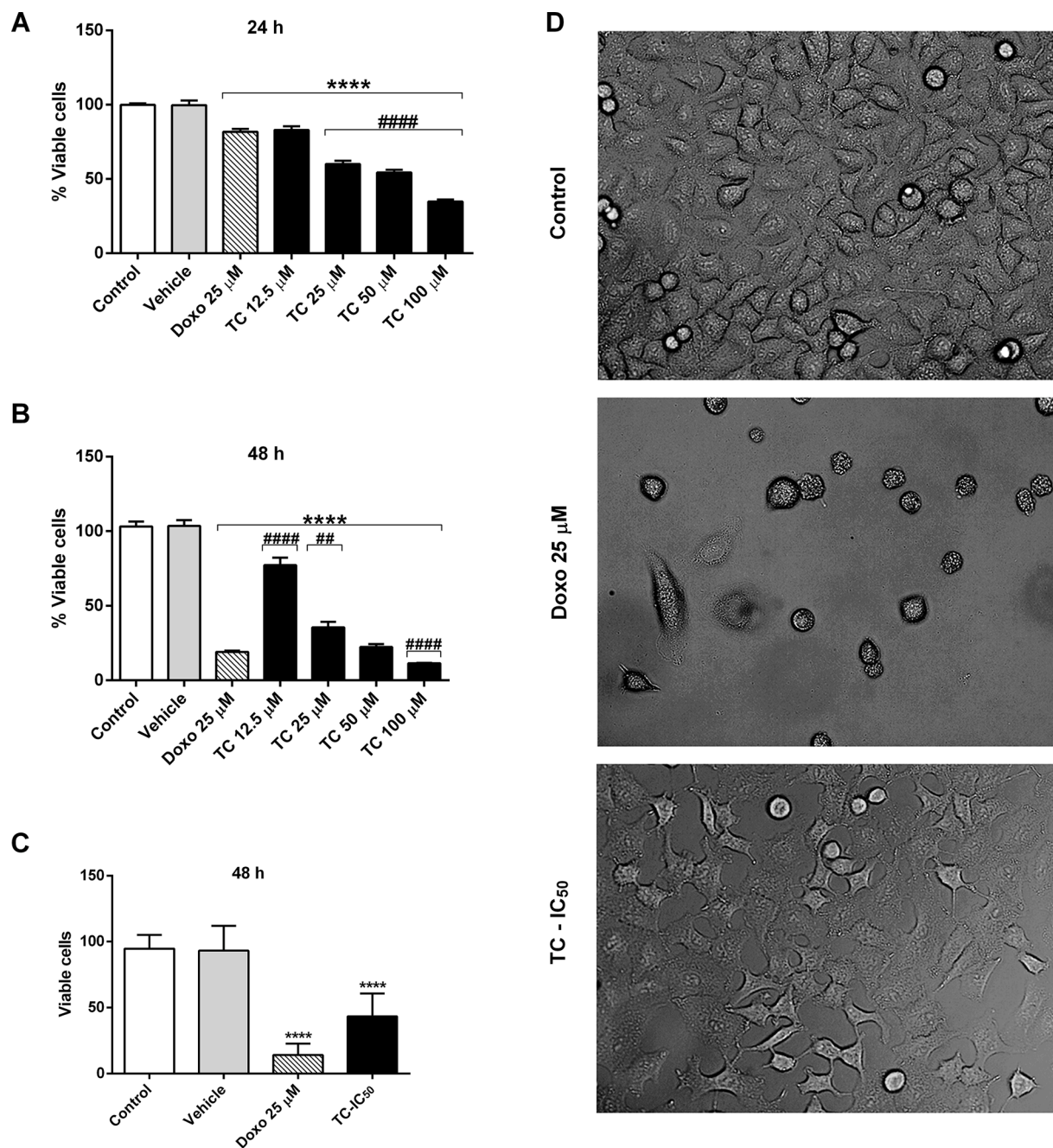


Fig. 2. Analysis of cell viability in the HCC HuH7.5 cell line. Treatment of HuH7.5 cells using TC at the concentrations of 12.5; 25; 50; 100 μM for 24 h (A) and 48 h (B) analyzed through MTT viability assay, trypan blue counting at 48 h (C), and quantification through image microscopy (D). Control (cells with DMEM medium), vehicle (0.01% DMSO), and Doxo (25 μM) (positive control). The values represent the mean \pm SEM of three different experiments performed in triplicate. **** Significant difference from control ($p \leq 0.0001$). ## Significant difference in relation to the positive control ($p \leq 0.01$) and **** ($p \leq 0.0001$).

Table 1

Detailed statistical analysis between the treatments and determination of 50% inhibitory concentration of *trans*-chalcone (TC-IC₅₀).

TC [μM]	24 h	48 h
12.5	a ($p = 0.0001$)	a ($p = 0.0001$)
25	b ($p = 0.0001$)	b ($p = 0.0001$)
50	b ($p = 0.0001$)	c ($p = 0.005$)
100	c ($p = 0.0001$)	d ($p = 0.01$)
IC ₅₀ (\pm SEM)	53 (\pm 0.04)	23.66 (\pm 0.02)

TC: *trans*-chalcone; μM : micromolar; h: hour; IC₅₀: 50% inhibitory concentration; SEM: stander error mean.

TC alters early ROS levels and promotes mitochondrial membrane depolarization

As *in vitro* treatment with TC has shown to have a direct effect on the HuH7.5 line, we sought to investigate its activity on these tumor cells. Initially, we verified whether the compound alters the levels of ROS. HuH7.5 cell TC-IC₅₀ treatment resulted in a higher early ROS production (four hours of treatment) comparing with the control group ($p \leq 0.005$) (Fig. 4A). After 48 h of treatment, despite a tendency for ROS production in treated cells, it proved not significant in relation to the control group (Fig. 4B).

It is known that significantly higher ROS can result in direct damage to mitochondria leading to changes in the functioning of this organelle.

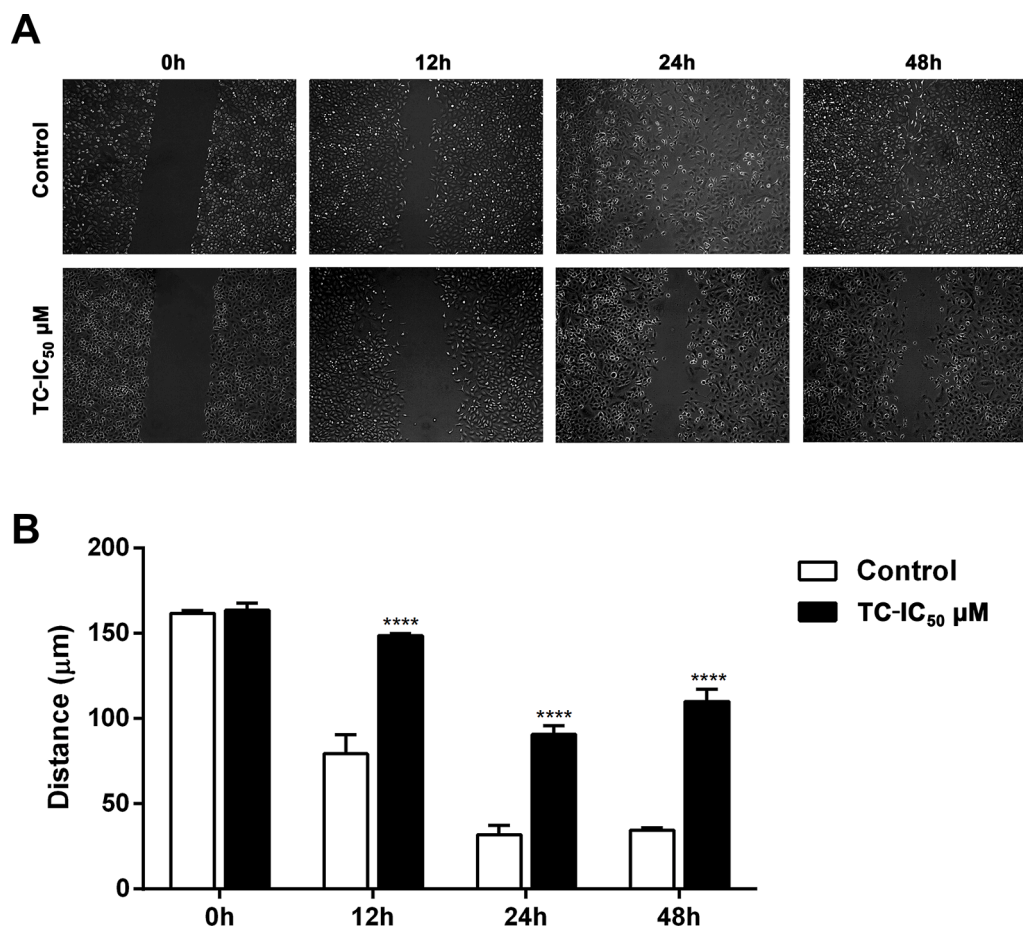


Fig. 3. Treatment with TC-IC₅₀ inhibited HuH7.5 cell migration. Scratch assay was performed to observe the effect of treatment on cell migration over time (0, 12, 24 and 48 h) (A) and the distance from the free area of these treated cells (B) was quantified. The values represent the mean \pm SEM of three different experiments performed in triplicate. Significant difference from **** ($p \leq 0.0001$) vs. control.

Therefore, we assessed the integrity of mitochondrial functioning by analyzing mitochondrial membrane potential through TMRE staining, which complexes with active mitochondria, since the significant loss of $\Delta\Psi_m$ renders exhausted cells with subsequent death. After 48 h of the HuH7.5 cell TC-IC₅₀ treatment, we found a reduction in the fluorescence intensity of the TMRE comparing with the control group in HuH7.5 ($p \leq 0.001$) (Fig. 4C), indicating loss of mitochondrial potential membrane similar to a positive control (CCCP treatment).

TC induces cell cycle arrest in the G0/G1 phase, increases p53 protein and decreases β -catenin levels in HuH7.5 cells

Additionally, we determined the distribution of HuH7.5 cells treated with TC-IC₅₀ at different stages of the cell cycle. Our findings showed that TC treatment results in changes in the percentage of cells according to the phases in the cell cycle. HuH7.5 cell TC-IC₅₀ treatment increased the percentage of G0/G1 phase cells ($p \leq 0.01$) and reduced the percentage of cells in S ($p \leq 0.05$) and G2/M ($p \leq 0.01$) phase when compared with the untreated cells (Fig. 5A, B). Taken together, these results demonstrated that TC induced the G0/G1 cell cycle arrest, consequently reducing the progression to cell division.

To verify the presence of proteins involved in tumorigenesis, we performed immunocytochemical markings of p53 and β -catenin on HuH7.5 cells. p53 is a tumor-suppressor gene that is mutated at codon 220 (Y220C) in HuH7-derived cell line, crucial to oncogenic cell activity (Zhao et al., 2018). Our results showed that control cells did not present p53 labeling, however, TC-IC₅₀ treatment restored p53 expression by significantly increasing the nuclear and cytoplasmic labeling of

the protein ($p \leq 0.01$) (Fig. 5C), reestablishing the control phenotype in which DNA binding capacity to p53 had been strongly suppressed. We also assessed the Wnt/ β -catenin pathway, which is mutated in HuH7.5 resulting in the activation of oncogenes, such as cyclin D1 and c-Myc. Results showed the occurrence of higher β -catenin labeling in untreated cells, which is suppressed by the TC-IC₅₀ treatment ($p \leq 0.01$) (Fig. 5D).

These data suggested that HuH7.5 cell TC-IC₅₀ treatment can effectively and significantly reverse activated/inactivated genes involved in the tumor mechanism.

TC induces autophagy process resulting in cell death

We also conducted apoptosis and autophagy analyses on these cells seeking to elucidate the possible mechanisms of death exerted by TC against the HuH7.5 cell line. Even though autophagy generally functions as a cell survival mechanism, the autophagic response to p53 activation has demonstrated important for p53-mediated cell death.

By marking autophagic vacuoles through MDC, we found that after 48 h of TC-IC₅₀ treatment, autophagic vacuole formation increased in relation to the untreated control ($p \leq 0.01$) (Fig. 6A). In turn, the assessment the phosphatidylserine (PS) expression as an apoptotic marker revealed that the TC-IC₅₀ treatment did not alter PS expression after 48 h of treatment (Fig. 6B).

Discussion

Given the lack of effective therapies for human HCC, especially at the advanced stages of the disease, it is particularly important to find

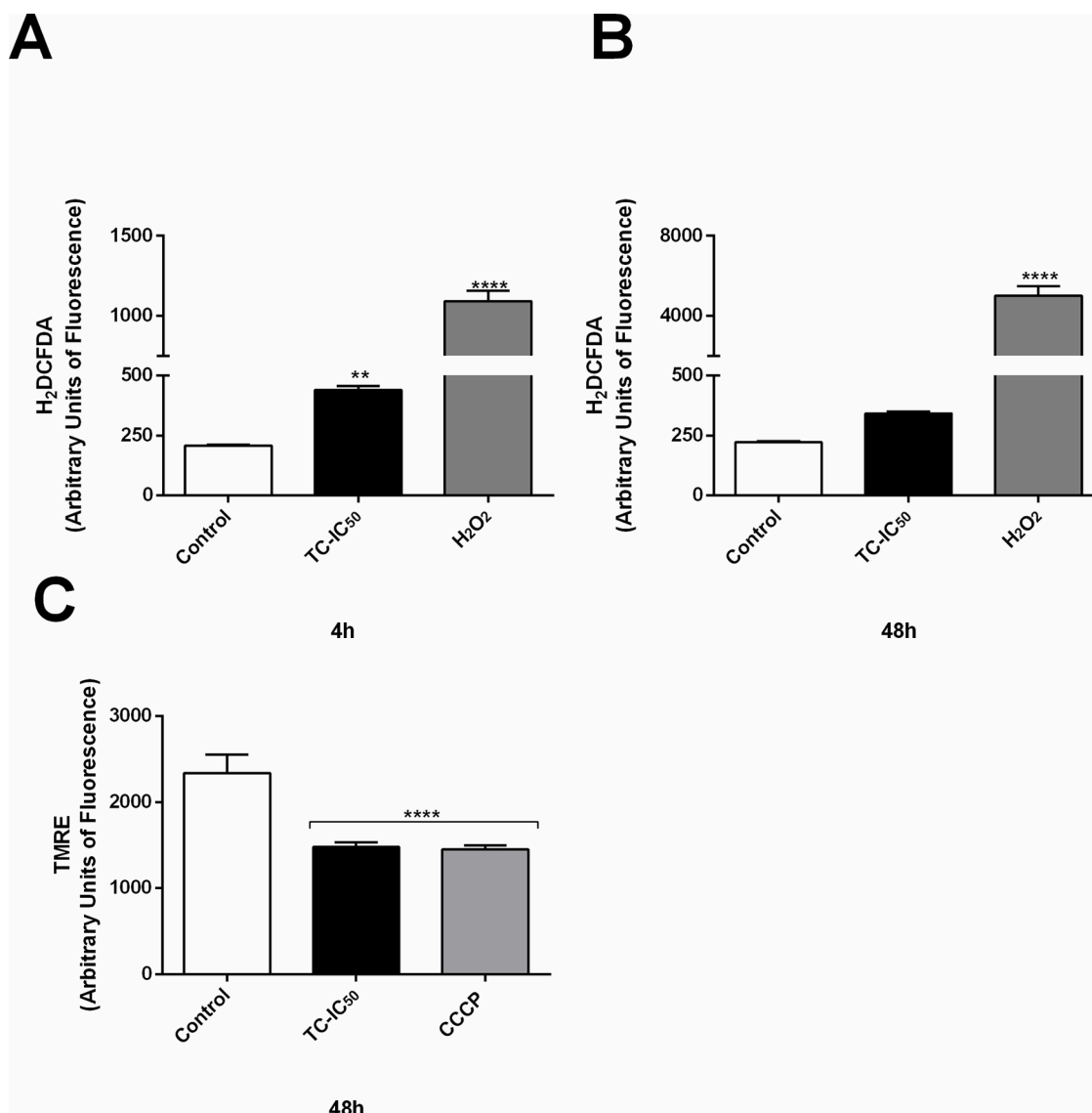


Fig. 4. ROS production and mitochondrial depolarization in HuH7.5 cells after treatment with TC-IC₅₀ (23.66 μ M). Cells were stained with H₂DCFDA probe and analyzed at 4 h (A) and 48 h (B) to determine ROS levels. TMRE assay for fluorimetric analysis of the $\Delta\Psi_m$ after 48 h (C). H₂O₂ and CCCP as positive controls. The values represent the mean \pm SEM of three different experiments performed in triplicate. ** Significant difference from control ($p \leq 0.01$), *** ($p \leq 0.001$) and **** ($p \leq 0.0001$).

improved therapeutic strategies for HCC. Therefore, several studies have focused on the discovery and development of new drugs based on natural products (Rayan et al., 2017). In this context, TC, a natural product that has already confirmed its antiproliferative properties in other types of tumor cells emerges as a potential compound in the treatment of liver tumor cell lines.

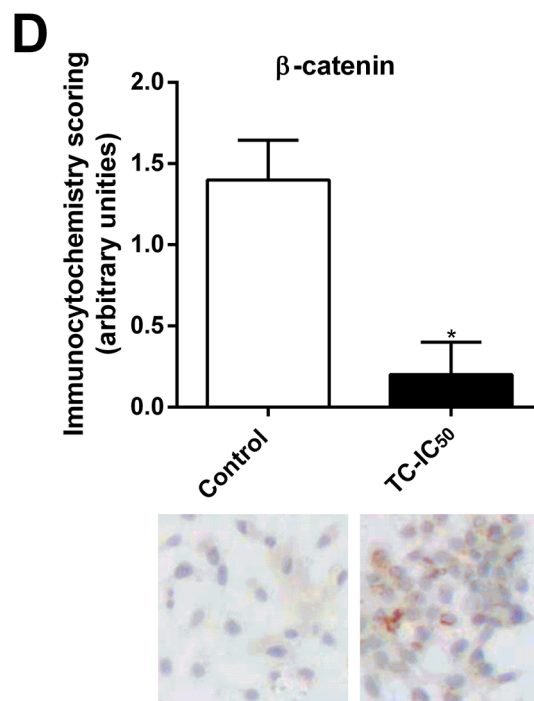
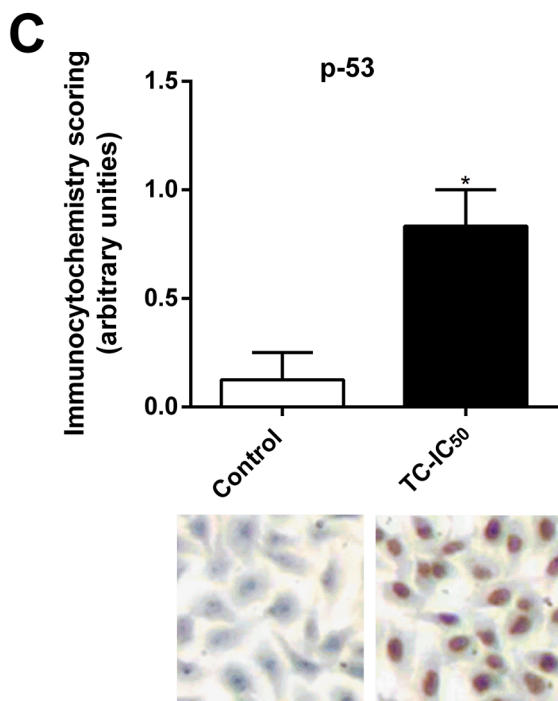
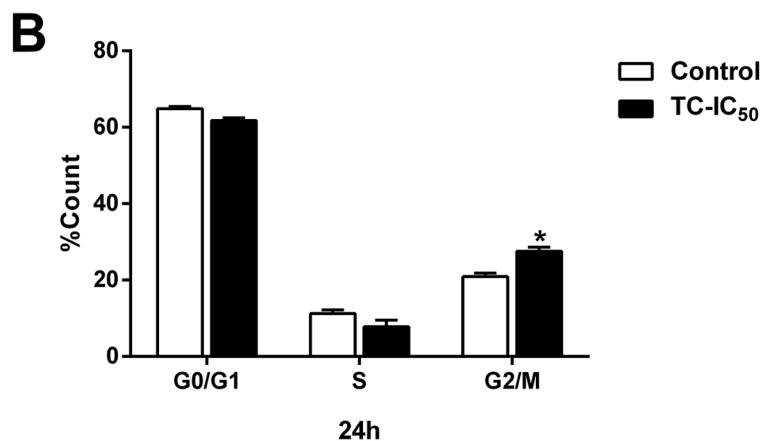
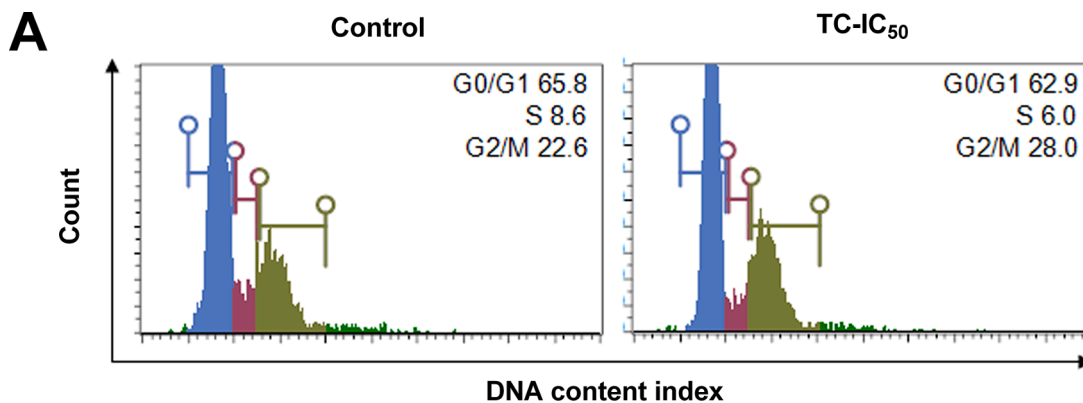
In this sense, our study sought to elucidate new perspectives of the TC- action mechanism against the *in vitro* human HCC HuH7.5 cell line. Data showed an effective TC-cytotoxic action in a dose- and time-dependent manner at low micromolar concentrations without causing toxicity to non-cancerous cells such as erythrocytes. TC treatment caused mitochondrial membrane damage, affecting the expression of tumor suppressor gene (p-53) and tumor developmental pathway (β -catenin) inducing cell death by autophagy. In addition, TC decreased HuH7.5 metastatic capacity affecting the migration/invasion capacity and the cell division progression of this cell type.

Anticancer activity of most natural products often acts by regulating the immune function, inducing apoptosis or autophagy, or inhibiting cell proliferation (reviewed in Rayan et al., 2017). Regarding the TC

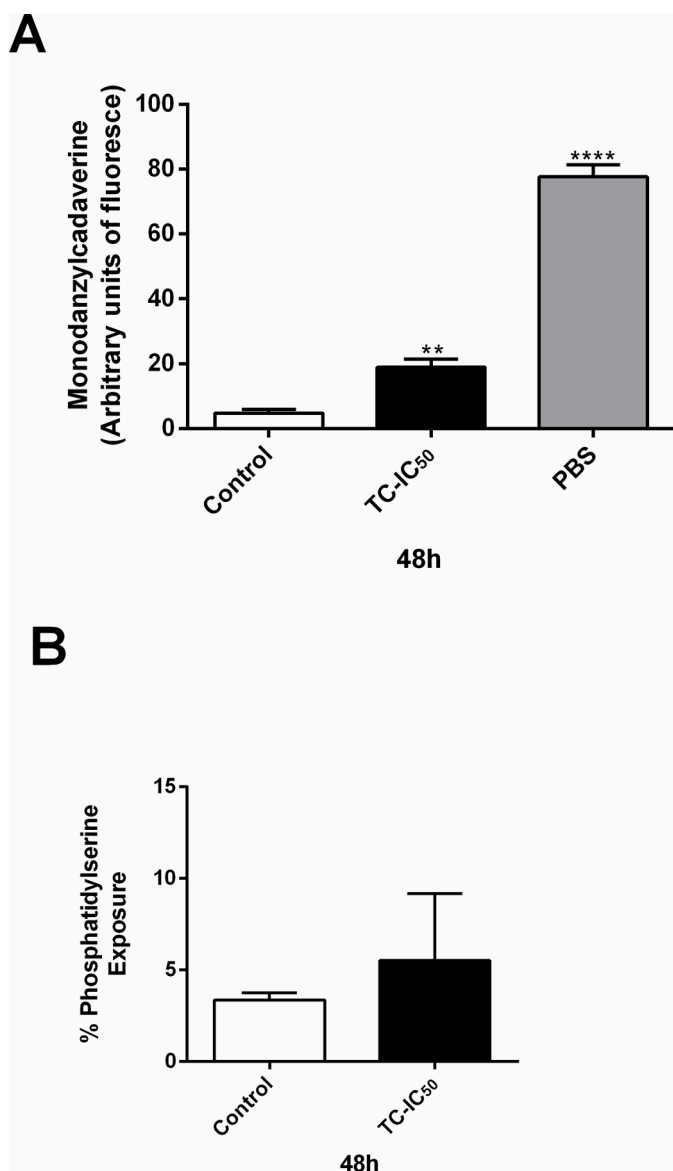
antitumor activity, some reports reveal the antiproliferative activity of TC against several different human tumor cell lines, such as T24 and HT-1376 (bladder cancer) (Shen et al., 2007), endometrial carcinoma Ishikawa lineage, MCF-7 and MDA-MD-231 (breast cancer) (Bortolotto et al., 2017; Mateeva et al., 2017), U2OS and SJSA-1 (osteosarcoma cells), HCT-116 (colon carcinoma), FaDu (epithelial cell line) (Silva et al., 2018, 2016), and 3T3 (murine fibroblasts) (Bortolotto et al., 2017). However, the literature brings no reports regarding the effect of TC on HuH7.5 cell lines.

This antiproliferative effect of TC was mainly found in the inhibition of the nuclear factor kappa B (NF- κ B) and upregulation of the tumor suppressor p53 gene (Bortolotto et al., 2017; Shen et al., 2007; Silva et al., 2018, 2016). It is well known that the p53 protein induces the p21 expression, which binds to cyclin E/Cdk2 and cyclin D/Cdk4 complexes to cause G1 arrest in the cell cycle, culminating in the regulation of apoptosis and autophagy (Chen, 2016). Corroborating with these data, such alterations on cell cycle were observed in our work.

While containing many mutations, as well as insertion or deletion of bases in the cell genome, it is worth observing that HuH7 cells also have



TC induces cell cycle arrest in G0/G1 and increases the staining of β-catenin and p53 proteins. HuH7.5 cells were treated with TC-IC₅₀ (23.66 μM) for 24 h and the cell cycle distribution by flow cytometry were plotted (A). Quantitative analyses of cells at different stages of the cell cycle were evaluated in 24 h (B). Immunocytochemical assay, after nuclear staining of proteins p53 (C) and β-catenin (D) were evaluated after 48 h of treatment. Immunocytochemistry score was classified as high positive (3+), positive (2+), low positive (1+) and negative (0). The values represent the mean ± SEM of three different experiments performed in triplicate. * Significant difference in control ($p \leq 0.01$) and ** ($p \leq 0.001$).



Presence of autophagic vacuoles and phosphatidylserine exposure on HuH7.5 cell line treated with TC for 48 h. Fluorescence intensity was quantified to determine autophagic vacuoles using the MDC marker (A). Quantitative analysis of the PS marking was evaluated in (B). PBS was used as a positive control. The values represent the mean \pm SEM of three different experiments performed in triplicate. ** Significant difference in control ($p \leq 0.01$) and **** ($p \leq 0.0001$).

somatic mutations, such as in the p53 cell cycle (Zhao et al., 2018). Cagatay and Ozturk (2002) also showed a perfect correlation between p53 gene mutation and aberrant accumulation of β -catenin protein in the HuH7 cell line.

In this context, our results demonstrated to have repaired the p53 pathway in which the HuH7.5 TC-IC₅₀ treatment enhanced the levels of p53, thus corroborating with (Silva et al., 2018, 2016), a study that found that the rescue of p53 activity in mutant p53 cancer cells induced the regression of U2OS, SJS-1, HCT-116, and FaDu cell lines. In addition, we observed β -catenin suppression in the TC-IC₅₀ treatment, which represents the first report on the action of TC on the Wnt/ β -catenin pathway, generally overactivated under pathological conditions such as HCC (Inagawa et al., 2002).

Interestingly, our data showed that the HuH7.5 treatment with TC-IC₅₀ did not induce apoptosis, a cell death often associated with high p53 expression over the period assessed (Chen, 2016). However, the

upregulation of p53 and Wnt/ β -catenin pathway has already been shown to be associated with autophagy, a process known as cellular recycling through the formation of autophagic vacuoles that allow programmed protein degradation and organelle turnover that contribute to the maintenance of cellular homeostasis (Moulder et al., 2018; Rabinowitz and White, 2010).

The role of autophagy in HCC remains controversial, as interference with the autophagic mechanism may promote or interrupt tumorigenesis (Mrakovcic and Fröhlich, 2018). Sun et al. (2013) showed that the role of autophagy in the occurrence and development of HCC is dependent on the context of liver cells. During the dysplastic phase in hepatocytes, basal autophagy acts as a suppressive tumor by removing newly damaged mitochondria and mutated cells, thus maintaining genomic stability. However, once a tumor is established, unbalanced autophagy will contribute to HCC cell survival under various stress conditions, in turn, promoting tumor growth.

Although autophagy is a physiological process with an inconclusive role in liver cancer, such phenomenon may be part of the events that result in autophagic cell death, type II programmed cell death, a form of non-apoptotic cell death mechanism (Scarlati et al., 2009). Recently, Martins et al. (2019) showed that the autophagy process, once associated with parallel damage in mitochondria and lysosomes, is an efficient way to induce cell death by autophagy. Our data corroborate this work by showing that HuH7.5 TC-IC₅₀ treatment generated an early production of ROS and mitochondrial damage through the mitochondrial membrane depolarization resulting in high and efficient cell death, which was verified by its cytotoxic effect through a trypan blue assay.

Mitochondrial depolarization caused by the TC treatment resulted in the loss of organelle integrity. Mitochondria are known to be hyperpolarized in tumors and modulate various biological functions, such as proliferation, differentiation, invasion, and metastasis (Zhang et al., 2019). Cancer metastasis is a complex process of cell spreading, which can be divided into migration, invasion, intravasation, survival in the circulation, extravasation, and metastatic colonization (Hanahan and Weinberg, 2000; Mina and Sledge, 2011). Migration and invasion represent the crucial steps for metastasis to be successful (Harlozinska, 2005). Our data suggested that TC-IC₅₀ treatment affected the ability of migration and invasion of HuH7.5 cells and may be a promising candidate for anti-metastasis use.

Conclusion

In conclusion, this work provided new insights on the in vitro TC-activity in human HCC HuH7.5 tumor cell line as a potential molecule for the development of new therapies to repair the p53 pathway and prevent the overexpression of Wnt/ β -catenin tumor development pathway, inducing cell cycle arrest in G0/G1 and autophagy cell death, decreasing the metastatic capacity of HuH7.5 cell line.

Taken together, our findings indicate that TC is a molecule to be investigated in further studies on anti-metastasis and antitumor activities in human hepatocellular carcinoma and can become a lead molecule for the design of new prototypes of more potent and selective antitumor compounds.

CRedit authorship contribution statement

Elaine da Silva Siqueira: Conceptualization, Methodology, Validation, Formal analysis, Investigation, Writing - original draft, Visualization. **Virgínia Márcia Concato:** Conceptualization, Methodology, Validation, Formal analysis, Investigation, Writing - original draft, Visualization. **Fernanda Tomiotto-Pellissier:** Formal analysis, Investigation, Writing - review & editing, Visualization, Validation, Data curation. **Taylon Felipe Silva:** Formal analysis, Investigation, Writing - review & editing, Visualization, Validation, Data curation. **Bruna Taciane da Silva Bortoleti:** Formal analysis, Investigation, Writing - review & editing, Visualization, Validation, Data curation. **Manoela Daiele**

Gonçalves: Formal analysis, Investigation, Writing - review & editing, Visualization, Validation, Data curation. **Idessania Nazareth Costa:** Resources, Data curation, Writing - review & editing, Supervision, Project administration, Funding acquisition. **Waldiceu Aparecido Verri Junior:** Resources, Data curation, Writing - review & editing, Supervision, Project administration, Funding acquisition. **Wander Rogério Pavanelli:** Resources, Data curation, Writing - review & editing, Supervision, Project administration, Funding acquisition. **Carolina Panis:** Resources, Data curation, Writing - review & editing, Supervision, Project administration, Funding acquisition. **Mário Sérgio Mantovani:** Resources, Data curation, Writing - review & editing, Supervision, Project administration, Funding acquisition. **Milena Menegazzo Miranda-Sapla:** Resources, Data curation, Writing - review & editing, Supervision, Project administration, Funding acquisition. **Ivete Conchon-Costa:** Resources, Data curation, Writing - review & editing, Supervision, Project administration, Funding acquisition.

Declaration of Competing Interest

Authors declare that they have no conflict of interest

Acknowledgments

Authors gratefully acknowledge Ivy Gobeti for helping with the English editing of the paper.

Funding

Not applicable.

References

- Aksöz, B.E., Ertan, R., 2011. Chemical and Structural Properties of Chalcones I. *J. Pharm. Sci.*
- Blandino, G., Valenti, F., Sacconi, A., Di Agostino, S., 2020. Wild type- and mutant p53 proteins in mitochondrial dysfunction: emerging insights in cancer disease. *Semin. Cell Dev. Biol.* <https://doi.org/10.1016/j.semcdb.2019.05.011>.
- Bortolotto, L.F.B., Barbosa, F.R., Silva, G., Bitencourt, T.A., Belebony, R.O., Baek, S.J., Marins, M., Fachin, A.L., 2017. Cytotoxicity of trans-chalcone and licochalcone A against breast cancer cells is due to apoptosis induction and cell cycle arrest. *Biomed. Pharmacother.* 85, 425–433. <https://doi.org/10.1016/j.biopha.2016.11.047>.
- Cagatay, T., Ozturk, M., 2002. p53 mutation as a source of aberrant β -catenin accumulation in cancer cells. *Oncogene* 21, 7971–7980. <https://doi.org/10.1038/sj.onc.1205919>.
- Chatterjee, S., Biswas, G., Chandra, S., Saha, G.K., Acharya, K., 2013. Apoptogenic effects of *Tricholoma giganteum* on Ehrlich's ascites carcinoma cell. *Bioprocess Biosyst. Eng.* 36, 101–107. <https://doi.org/10.1007/s00449-012-0765-6>.
- Chen, J., 2016. The cell-cycle arrest and apoptotic functions of p53 in tumor initiation and progression. *Cold Spring Harb. Perspect. Med.* 6. <https://doi.org/10.1101/cshperspect.a026104>.
- Concato, V.M., Tomiotto-Pellissier, F., Silva, T.F., Gonçalves, M.D., Bortoleti, B.T.da S., Detoni, M.B., Siqueira, E.da S., Rodrigues, A.C.J., Schirmann, J.G., Barbosa-Dekker, A., de, M., Costa, I.N., Conchon-Costa, I., Miranda-Sapla, M.M., Mantovani, M.S., Pavanelli, W.R., 2020. 3,3',5,5'-tetramethoxybiphenyl-4,4' diol induces cell cycle arrest in G2/M phase and apoptosis in human non-small cell lung cancer A549 cells. *Chem. Biol. Interact.* 326, 109133 <https://doi.org/10.1016/j.cbi.2020.109133>.
- Gonçalves, M.D., Bortoleti, B.T.S., Tomiotto-Pellissier, F., Miranda-Sapla, M.M., Assolini, J.P., Carlotto, A.C.M., Carvalho, P.G.C., Tudisco, E.T., Urbano, A., Ambrósio, S.R., Hirooka, E.Y., Simão, A.N.C., Costa, I.N., Pavanelli, W.R., Conchon-Costa, I., Arakawa, N.S., 2018. Dehydroabietic acid isolated from *Pinus elliottii* exerts in vitro antileishmanial action by pro-oxidant effect, inducing ROS production in promastigote and downregulating Nrf2/ferritin expression in amastigote forms of *Leishmania amazonensis*. *Fitoterapia* 128, 224–232. <https://doi.org/10.1016/j.fitote.2018.05.027>.
- Hanahan, D., Weinberg, R.A., 2000. The hallmarks of cancer. *Cell.* [https://doi.org/10.1016/S0092-8674\(00\)81683-9](https://doi.org/10.1016/S0092-8674(00)81683-9).
- Harlozinska, A., 2005. Progress in molecular mechanisms of tumor metastasis and angiogenesis. *Anticancer Res.* 25, 3327–3333.
- Inagawa, S., Itabashi, M., Adachi, S., Kawamoto, T., Hori, M., Shimazaki, J., Yoshimi, F., Fukao, K., Y, S.F., 2002. Expression and Prognostic Roles Of-Catenin in Hepatocellular Carcinoma: Correlation with Tumor Progression and Postoperative Survival.
- Martins, W.K., Santos, N.F., Rocha, C., de, S., Bacellar, I.O.L., Tsubone, T.M., Viotto, A.C., Matsukuma, A.Y., Abrantes, A.B., d., P., Siani, P., Dias, L.G., Baptista, M.S., 2019. Parallel damage in mitochondria and lysosomes is an efficient way to photoinduce cell death. *Autophagy* 15, 259–279. <https://doi.org/10.1080/15548627.2018.1515609>.
- Mateeva, N., Eyunni, S.V.K., Redda, K.K., Ononju, U., Hansberry, T.D., Aikens, C., Nag, A., 2017. Functional evaluation of synthetic flavonoids and chalcones for potential antiviral and anticancer properties. *Bioorganic Med. Chem. Lett.* 27, 2350–2356. <https://doi.org/10.1016/j.bmlcl.2017.04.034>.
- Mina, L.A., Sledge, G.W., 2011. Rethinking the metastatic cascade as a therapeutic target. *Nat. Rev. Clin. Oncol.* 8, 325–332. <https://doi.org/10.1038/nrclinonc.2011.59>.
- Moulder, D.E., Hatoum, D., Tay, E., Lin, Y., McGowan, E.M., 2018. The roles of p53 in mitochondrial dynamics and cancer metabolism: the pendulum between survival and death in breast cancer? *Cancers (Basel)* 10. <https://doi.org/10.3390/cancers10060189>.
- Mrakovcic, M., Fröhlich, L.F., 2018. P53-mediated molecular control of autophagy in tumor cells. *Biomolecules.* <https://doi.org/10.3390/biom8020014>.
- New Global Cancer Data: GLOBOCAN 2018 | UICC [<https://www.uicc.org/new-global-cancer-data-globocan-2018>], n.d.
- Bonakdar, A.P.S., Vafaei, F., Farokhpour, M., Nasr Esfahani, M.H., Massah, A.R., 2017. Synthesis and Anticancer Activity Assay of Novel Chalcone-Sulfonamide Derivatives. *Iran. J. Pharm. Res. IJPR* 16, 565–568.
- Rabinowitz, J.D., White, E., 2010. Autophagy and metabolism. *Science.* <https://doi.org/10.1126/science.1193497>.
- Rayan, A., Raijn, J., Falah, M., 2017. Nature is the best source of anticancer drugs: indexing natural products for their anticancer bioactivity. *PLoS ONE* 12. <https://doi.org/10.1371/journal.pone.0187925>.
- Scarlati, F., Granata, R., Meijer, A.J., Codogno, P., 2009. Does autophagy have a license to kill mammalian cells? *Cell Death Differ.* <https://doi.org/10.1038/cdd.2008.101>.
- Shen, K.H., Chang, J.K., Hsu, Y.L., Kuo, P.L., 2007. Chalcone arrests cell cycle progression and induces apoptosis through induction of mitochondrial pathway and inhibition of nuclear factor kappa B signalling in human bladder cancer cells. *Basic Clin. Pharmacol. Toxicol.* 101, 254–261. <https://doi.org/10.1111/j.1742-7843.2007.00120.x>.
- Silva, G., Marins, M., Chaichanasak, N., Yoon, Y., Fachin, A.L., Pinhanelli, V.C., Regasini, L.O., dos Santos, M.B., Ayusso, G.M., Marques, B., de, C., Wu, W.W., Phue, J.-N., Shen, R.-F., Baek, S.J., 2018. Trans-chalcone increases p53 activity via DNAJB1/HSP40 induction and CRM1 inhibition. *PLoS ONE* 13. <https://doi.org/10.1371/journal.pone.0202263> e0202263.
- Silva, G., Marins, M., Fachin, A.L., Lee, S.H., Baek, S.J., 2016. Anti-cancer activity of trans-chalcone in osteosarcoma: involvement of Sp1 and p53. *Mol. Carcinog.* 55, 1438–1448. <https://doi.org/10.1002/mc.22386>.
- Sim, H.W., Knox, J., 2018. Hepatocellular carcinoma in the era of immunotherapy. *Curr. Probl. Cancer.* <https://doi.org/10.1016/j.cuprob.2017.10.007>.
- Sun, K., Guo, X.L., Zhao, Q.D., Jing, Y.Y., Kou, X.R., Xie, X.Q., Zhou, Y., Cai, N., Gao, L., Zhao, X., Zhang, S.S., Song, J.R., Li, D., Deng, W.J., Li, R., Wu, M.C., Wei, L.X., 2013. Paradoxical role of autophagy in the dysplastic and tumor-forming stages of hepatocarcinoma development in rats. *Cell Death Dis.* 4, e501. <https://doi.org/10.1038/cddis.2013.35>.
- Wands, J.R., Kim, M., 2014. WNT/ β -catenin signaling and hepatocellular carcinoma. *Hepatology* 60, 452–454. <https://doi.org/10.1002/hep.27081>.
- Xue, W., Zender, L., Miething, C., Dickins, R.A., Hernandez, E., Krizhanovskiy, V., Cordon-Cardo, C., Lowe, S.W., 2007. Senescence and tumour clearance is triggered by p53 restoration in murine liver carcinomas. *Nature* 445, 656–660. <https://doi.org/10.1038/nature05529>.
- Zhang, L., Li, S., Wang, R., Chen, C., Ma, W., Cai, H., 2019. Anti-tumor effect of LATS2 on liver cancer death: role of DRP1-mediated mitochondrial division and the Wnt/ β -catenin pathway. *Biomed. Pharmacother.* 114. <https://doi.org/10.1016/j.biopha.2019.108825>.
- Zhao, Y., Chen, Y., Hu, Y., Wang, J., Xie, X., He, G., Chen, H., Shao, Q., Zeng, H., Zhang, H., 2018. Genomic alterations across six hepatocellular carcinoma cell lines by panel-based sequencing. *Transl. Cancer Res.* 7, 231–239. <https://doi.org/10.21037/20035>.